Fast Fat Suppression Technique for Adaptive 3D Radial MRI Based on Multidimensional Golden Means

P. Siegler[1], R. W-C. Chan[2], E. Ramsay[1], and D. B. Plewes[1]

[1]Imaging Research, Sunnybrook Health Sciences Centre, Toronto, Ontario, Canada, [2]Medical Biophysics, University of Toronto, Toronto, Ontario, Canada

INTRODUCTION

Adaptive sampling of *k*-space allows the reconstruction of images with various spatial and temporal resolutions from the same data set and is therefore suitable for dynamic MRI [1,2]. Golden-angle radial *k*-space sampling achieves this flexibility in-plane with relatively uniform angular sampling distribution for any time interval using samples incremented by the golden angle, $\phi = (\sqrt{5}-1)/2 \cdot 180° \approx 111.25°$ [3]. To achieve a similar sampling pattern in 3D *k*-space, this was extended to 3D projection reconstruction (PR) based on multidimensional golden means ("golden 3D-PR") [4].

The uniform sampling of *k*-space over time with 2D radial MRI, can be combined with the *k*-space-weighted image contrast (KWIC) technique [5] to compensate for respiratory motion [6]. As the periodic time intervals in golden angle MRI show an approximately uniform coverage of *k*-space, uniform filling of KWIC regions in *k*-space over time is possible.

This fact is also valid for golden 3D- PR and is used here for fast fat suppression using partial fat saturation [7], where the KWIC regions are filled depending on the time interval between the current projection and the last projection with a fat saturation pulse.

MATERIALS AND METHODS

In golden 3D PR [4], the first of the higher dimensional golden means (0.4656) determined the k_z location while the second (0.6823) determined the in-plane angle of the 3D radial projections. For the partial fat saturation [6], each R_{fat}-th projection of the golden angle radial scan was preceded by a fat saturation pulse. Using KWIC processing [5], the most central *k*-space sphere (radius of 10 *k*-space positions) around the *k*-space center was filled with the projections which had been acquired a maximum of $R_{fat}/4$ repetitions after a fat saturation pulse. In the shell around the central *k*-space sphere (outer radius of 20 *k*-space positions) all the projections acquired a maximum of $R_{fat}/2$ repetitions after a fat saturation pulse were used. For the rest of *k*-space all acquired projections were used.

The experiments were performed on a high-resolution phantom with a fat compartment. A whole body 1.5T MR scanner (GE Signa Excite) and a fast 3D spoiled gradient echo (fast 3D SPGR) golden PR sequence (T_E=4.2ms, T_R=9.725ms without fat saturation pulse, T_R=19.432ms with fat saturation pulse and FOV = 216×216×216mm^3) were used for imaging.

- Fat recovery with different excitation angles:
  Data sets were acquired with the 3D golden angle approach (32,000 projections) and R_{fat}=32 but varying flip angle α. To show the different levels of fat recovery with the different excitation angles, sub-data sets of all the projections acquired during the same repetition after the fat saturation pulse (1,000 projections) were created. The ratio of the mean water and the mean fat signal, both averaged over a region of interest, were determined. For α=9°, KWIC was applied on a data-set with 32,000 projections used for reconstruction.
- Different fat saturation ratios:
  Using α=9°, partial fat saturated data sets were acquired with different fat saturation ratios R_{fat}. In order to achieve fixed scan-times of 330s and 11s, the number of projections used for reconstruction was varied with R_{fat}. In addition, fully fat saturated 3D golden angle data sets with these fixed scan-times were acquired and reconstructed.

RESULTS

As with reordered fat saturation, the choice of flip angle strongly influenced the recovery of the fat signal during the repetitions after a fat saturation pulse (Fig.1). For R_{fat}=32, an excitation angle of α=9° results in the best water to fat ratios, whereas with higher flip angles the fat recovered more quickly and even overtook the water signal. In the case of α=5° the important first repetitions, which with KWIC would be placed in the central *k*-space region, showed lower fat saturation levels.

The partial fat saturation alone achieved a reduction of the fat signal (Fig. 2a). With KWIC, fat suppression could be further improved (Fig 2b).

For the longer scan-time tested (330s – left column of Fig.3), the proposed technique gave fat suppression comparable to full fat saturation. The fat signal increased with time between fat saturation pulses. For the shorter scan-time, the proposed technique allowed more projections to be included in the reconstruction, resulting in a noticeable reduction of undersampling artifacts.

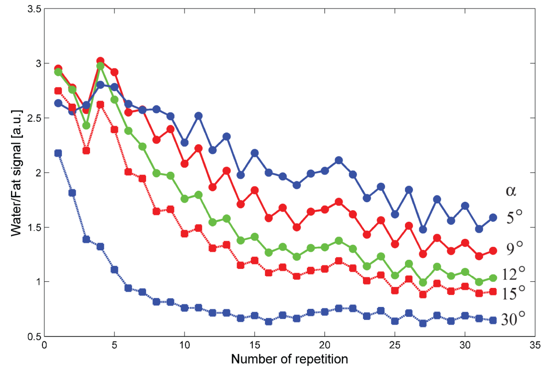

Figure 1: Ratio of the average water signal to the average fat signal as a function of the number of repetitions after the fat saturation pulse for different flip angles α. The rough curves for the small α are caused by undersampling artifacts inside the low fat signal.

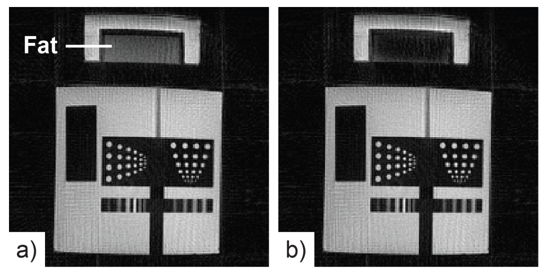

Figure 2: One slice through the 3D data set acquired with α=9° and R_{fat}=32. a) If all projections are used for reconstruction, fat signal remains in the final images. b) KWIC achieves improved fat saturation.

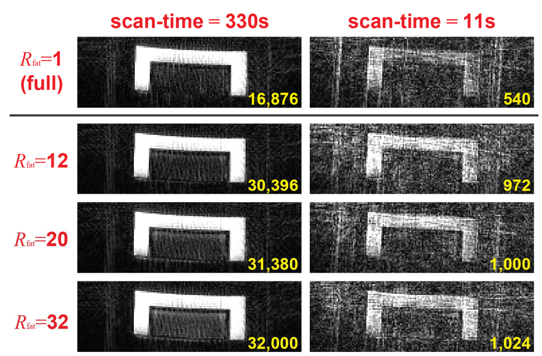

Figure 3: Comparison of fully fat saturated golden angle PR and KWIC partial fat saturated golden angle PR with different R_{fat}. Two different time resolutions were considered by varying the number of projections (right corner of each image) used for reconstruction.

DISCUSSION AND CONCLUSIONS

The periodic order of the partial fat saturation pulses in partial fat saturation segments the acquired golden 3D-PR data-set into sub-sets with equal fat saturation levels, which covers *k*-space with approximately uniformity. KWIC can therefore be successfully used to combine golden 3D-PR with partial fat saturation. For images reconstructed with high number of projections, the resulting fat suppression is slightly degraded compared to a fully fat saturated golden 3D-PR. However, the shorter scan-time of the new technique can be used to increase the number of projections in a given time interval, thus allowing the reconstruction of fat suppressed images at very high temporal resolution.

REFERENCES

[1] Rasche V, et al. MRM 1995;34:754-61 [2] Peters DC, et al. MRM 2000;43:91-101 [3] Winkelmann S, et al. IEEE TMI 2007;26:68-76 [4] Chan RWC, et al. MRM 2008 in press [5] Song HK, et al. MRM 2004;52:815-24 [6] Lin W, et al. MRM 2008;60:1135-46 [7] Desmond KL, et al. JMRI 2007;25:1293-8